# Reduction of 1,2-Bis[(2,6-diisopropylphenyl)imino]acenaphthene (dpp-bian) with Alkali Metals − A Study of the Solution Behaviour of (dpp-bian)$^{n-}$[M$^+$]$_n$ (M = Li, Na; $n$ = 1−4) with UV/Vis, ESR and $^1$H NMR Spectroscopy

**Igor L. Fedushkin,*[a] Alexandra A. Skatova,[a] Valentina A. Chudakova,[a] Vladimir K. Cherkasov,[a] Georgy K. Fukin,[a] and Mikhail A. Lopatin[a]**

**Keywords:** Lithium / Sodium / Bis(imino)acenaphthene / Polyanions

An excess of lithium or sodium in diethyl ether consistently reduces 1,2-bis[(2,6-diisopropylphenyl)imino]acenaphthene (dpp-bian) to the mono-, di-, tri- and tetraanion, (dpp-bian)$^{n-}$[M$^+$]$_n$ (M = Li, Na; $n$ = 1–4). The process of reduction is easily observed by the change in colour of the solution, on going from the neutral ligand (yellow) to the monoanion (red), the dianion (green for Na or Li in $Et_2O$; dark blue, followed by green, for Li in TMEDA), the trianion (brown) and the tetraanion (red-brown). In each reduction the maximum of the absorption, caused by electron transition from the HOMO of the respective form (dpp-bian)$^{n-}$ ($n$ = 1–4), is shifted to the long-wavelength region in comparison to the previously reduced state. The disproportionation reactions (dpp-bian)$^{1-}$ → (dpp-bian)$^0$ + (dpp-bian)$^{2-}$ and (dpp-bian)$^{2-}$ → (dpp-bian)$^{1-}$ + (dpp-bian)$^{3-}$ take place in solution along with the reduction process, thus causing the presence of three reduced forms of the ligand at the same time in the first and second stages of the reduction. Paramagnetic (dpp-bian)$^{1-}$ and (dpp-bian)$^{3-}$ are characterised by ESR spectroscopy. For the diamagnetic forms (dpp-bian)$^{2-}$ and (dpp-bian)$^{4-}$ $^1$H NMR spectra were recorded. The complex [Li$^+$(dpp-bian)(TMEDA)] (**1**), which formed from the initial stage of the reduction of dpp-bian with lithium metal in TMEDA, was isolated in a crystalline form and its molecular structure was determined by single-crystal X-ray diffraction.



## Introduction

Within the last few years 1,2-bis[(2,6-diisopropylphenyl)imino]acenaphthene (dpp-bian) began to be used widely in coordination chemistry of transition metals.[1] Several interesting chemical reactions of metal complexes based on this ligand were reported. Until recently only complexes of transition metals and only with the neutral dpp-bian ligand were studied. These complexes are active as catalysts in alkyne hydrogenation[2a], C−C[2b] and C−Sn[2c] bond formation, and especially in olefin polymerisation.[3] We have reported on the synthesis, isolation of crystals and detailed characterisation of the magnesium and calcium complexes with the dpp-bian dianion, (dpp-bian)$^{2-}$M$^{2+}$(L)$_n$ (M = Mg, L = THF, $n$ = 2, 3 and L = Py, $n$ = 3; M = Ca, L = THF, $n$ = 3, 4).[4] These Mg and Ca complexes are easy to synthesise by direct reduction of the ligand with metallic magnesium or calcium. The use of sodium metal has allowed the reduction of dpp-bian leading to the formation of the dianion and also the tetraanion. Thus, sodium salts of mono-, di-, tri- and tetraanions of the ligand, [Na$^+$(dpp-bian)$^-$]$_2$, [Na$^+_2$(Et$_2$O)$_3$(dpp-bian)$^{2-}$], [Na$^+_3$(Et$_2$O)$_2$(dpp-bian)$^{3-}$]$_2$, [Na$^+_4$(THF)$_4$(dpp-bian)$^{4-}$]$_2$, were isolated in crystalline form and characterised by single-crystal X-ray diffraction.[5] Thus, for the first time four anionic forms of a single ligand were isolated on a preparative scale and characterised by single-crystal X-ray structure analysis. At present one of our objectives is to use these sodium salts for synthesis of other non-transition metal complexes, which in turn, can be used as reducing agents of various classes of organic substrates, working over a wide range of the redox potentials.

To find an optimal synthetic approach to other metal complexes by metathetical reactions using the sodium salts (dpp-bian)$^{n-}$(Na$^+$)$_n$ ($n$ = 1−4), more insight into their solution behaviour is needed. Therefore, we started the UV/Vis and ESR spectroscopic study of (dpp-bian)$^{n-}$(Na$^+$)$_n$ ($n$ = 1−4) in solution. We also report here on the solution behavior of the lithium salts (dpp-bian)$^{n-}$(Li$^+$)$_n$ ($n$ = 1−4) prepared in situ in both diethyl ether and TMEDA as well as the solid-state molecular structure of the TMEDA adduct [Li$^+$(dpp-bian)$^-$(TMEDA)] (**1**).

[a] G. A. Razuvaev Institute of Organometallic Chemistry of Russian Academy of Sciences,
Russian Federation, Tropinina 49, 603950 Nizhny Novgorod GSP-445,
Fax: (internat.) + 7-8312-661-497
E-mail: igorfed@imoc.sinn.ru

  **DOI: 10.1002/ejic.200300351** 

## Results and Discussion

### Reduction of dpp-bian with Sodium and Lithium − The Solution UV/Vis Spectroscopy

In general, a solution of the dpp-bian ligand was added into an ampoule which contained the appropriate alkali metal and was connected to the spectroscopic cell. Then the ampoule was sealed off under vacuum. On shaking the ampoule for several hours, a colour change was observed and monitored by UV/Vis spectroscopy. Figure 1 represents the electronic absorption spectra of $[Na^+_n(dpp\text{-}bian)^{n-}]$ ($n$ = 1−4) obtained by reduction of dpp-bian with sodium metal in diethyl ether. The curves 1−9 reflect the change of spectra in a chronological sequence. The reduction is completed within 6 h upon intense shaking at room temperature. The neutral ligand exhibits an absorption at 420 nm, which corresponds to a yellow solution. Over the course of reduction the colour of the solution becomes darker, the band of absorption of the initial ligand gradually disappears, and the absorption of the radical anion $(dpp\text{-}bian)^-$ (435, 460 and 495 nm) (Figure 1, a, spectrum 1) becomes visible. As the reduction proceeds, the absorption band of $(dpp\text{-}bian)^-$ is lowered again and the absorption of the dianion (640 nm) is enhanced (Figure 1, a, spectrum 2). Spectrum 3 (Figure 1, a) shows the absorption of the dianion (640 nm) becoming more intensive and indicates the prevalence of the dianion in solution. The compound $[Na_2(Et_2O)_3(dpp\text{-}bian)]$, isolated in crystalline form,[5] exhibits the same spectrum. Figure 1 (b) reflects changes on going from $(dpp\text{-}bian)^{2-}$ to $(dpp\text{-}bian)^{3-}$. The absorption at 840 nm indicates the formation of the trianion $[Na^+_3(dpp\text{-}bian)^{3-}]$. As seen from Figure 1 (a and b), three reduced forms of the ligand are present at the same time in solution. This may be explained by the disproportionation: $(dpp\text{-}bian)^{1-} \rightarrow (dpp\text{-}bian)^0 + (dpp\text{-}bian)^{2-}$ and $(dpp\text{-}bian)^{2-} \rightarrow (dpp\text{-}bian)^{1-} + (dpp\text{-}bian)^{3-}$. Upon further reduction of $(dpp\text{-}bian)^{3-}$ with sodium the absorption of the trianion (840 nm) disappears (Figure 1, c). Spectrum 9 in Figure 1 (c) indicates the complete reduction of the ligand to the tetraanion. The tri- and tetraanions of the ligand show similar absorbance in the wavelength region (400−600 nm), but differ in the region of 700−1100 nm. It should be noted that this difference cannot be visually observed. Therefore, it is difficult to distinguish the colour of solutions of the tri- and tetraanions. Taking into account the observation that the absorption of every next reduced form has a lower absorption compared to that of the previous form, one can suggest that the absorption of the tetraanion, which originates from the electron transfer from the HOMO, is shifted into the near IR region. Although there is no isosbestic point in spectra 7−9, one can conclude that the disproportionation process $(dpp\text{-}bian)^{3-} \rightarrow (dpp\text{-}bian)^{2-} + (dpp\text{-}bian)^{4-}$ does not take place because of the absence of the absorption of the dianion (Figure 1, c).

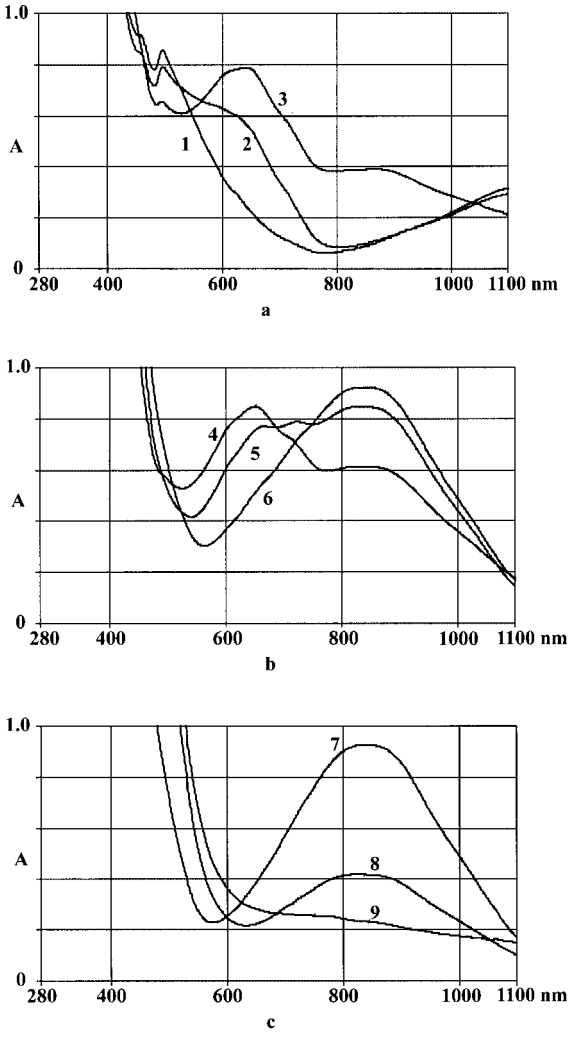


Figure 1. UV/Vis spectra of $(dpp\text{-}bian)^{n-}Na^+_n$ ($n$ = 1−4) in $Et_2O$ ($10^{-3}$ mol/L) in the Pyrex cell (3.5 mm): (a) $(dpp\text{-}bian) \rightarrow (dpp\text{-}bian)^-$, (b) $(dpp\text{-}bian)^- \rightarrow (dpp\text{-}bian)^{2-} \rightarrow (dpp\text{-}bian)^{3-}$, (c) $(dpp\text{-}bian)^{3-} \rightarrow (dpp\text{-}bian)^{4-}$; the curves **1−9** reflect the change of spectra in a chronological sequence

The process of the reduction of the dpp-bian ligand with lithium metal was also investigated by electron absorption spectroscopy. The spectra, which correspond to the intermediate reduced forms of the ligand, are presented in Figure 2. Spectra 1−3 indicate the consecutive transformation of the radical anion $(dpp\text{-}bian)^-$ to the dianion $(dpp\text{-}bian)^{2-}$ (432, 468, 503 nm and 595, 650 nm, respectively). In spectrum 2 the simultaneous presence of the three forms in solution is clearly visible. The trianion $(dpp\text{-}bian)^{3-}$ has a maximum at 718 nm, which confirms the dissproportionation of the dianion to the radical anion and trianion. Figure 2 (b) reflects a gradual transition of $(dpp\text{-}bian)^{2-}$ into $(dpp\text{-}bian)^{3-}$ (718 and 780 nm). Spectrum 6 corresponds to a solution in which the $(dpp\text{-}bian)^{3-}$ form is dominant. Figure 2 (c) shows changes in solution on going from the trianion to the tetraanion. The existence of the isosbestic point in spectra 7−9 indicates that the trianion is completely converted by lithium under electron transfer into the tetranion without any side reactions (disproportionation etc.).

Upon reduction of dpp-bian with lithium in a diluted diethyl ether solution, we observed at the initial stages an appearance of an intense blue colour on cooling to about

  

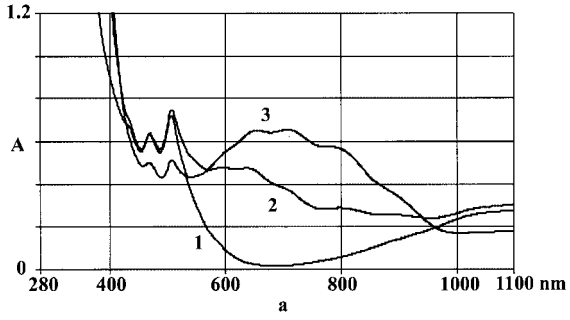


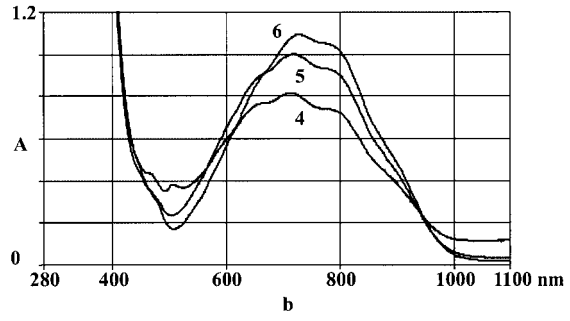


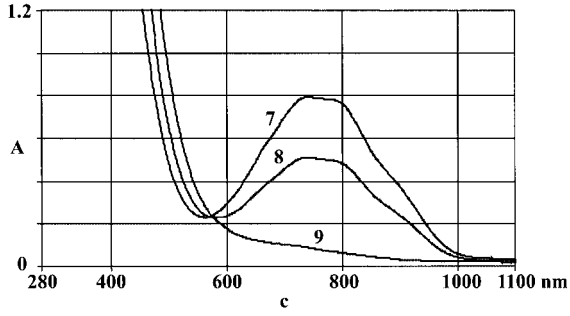


Figure 2. UV/Vis spectra of $(dpp\text{-}bian)^{n-}Li^{+}_{n}$ ($n = 1-4$) in $Et_2O$ ($10^{-3}$ mol/L) in the Pyrex cell (3.5 mm): (a) (dpp-bian) → (dpp-bian)$^{-}$, (b) (dpp-bian)$^{-}$ → (dpp-bian)$^{2-}$ → (dpp-bian)$^{3-}$, (c) (dpp-bian)$^{3-}$ → (dpp-bian)$^{4-}$; the curves **1**−**9** reflect the change of spectra in a chronological sequence

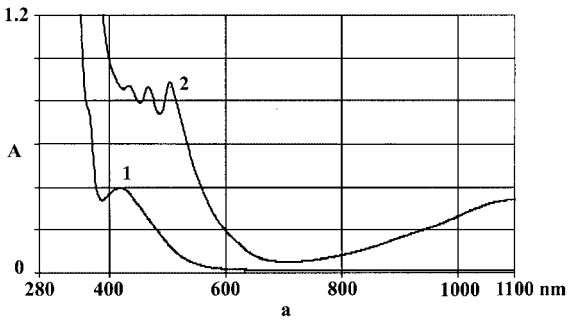


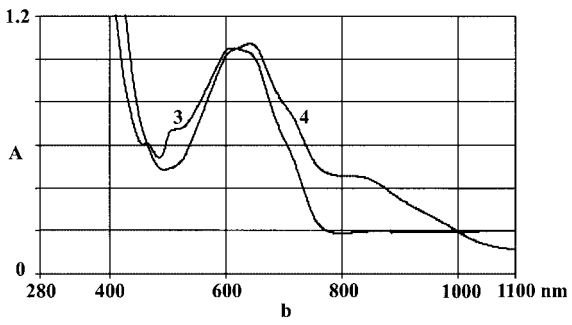


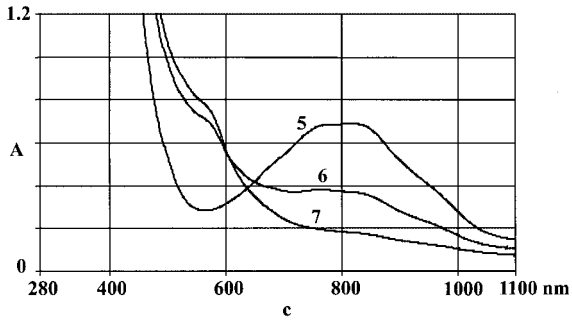


Figure 3. UV/Vis spectra of $(dpp\text{-}bian)^{n-}Li^{+}_{n}$ ($n = 1-4$) in TMEDA ($10^{-3}$ mol/L) in a Pyrex cell (3.5 mm): (a) (dpp-bian) → (dpp-bian)$^{-}$, (b) (dpp-bian)$^{-}$ → (dpp-bian)$^{2-}$ → (dpp-bian)$^{3-}$, (c) (dpp-bian)$^{3-}$ → (dpp-bian)$^{4-}$; the curves **1**−**7** reflect the change of spectra in a chronological sequence

−50 °C. It was neither observed in the case of sodium nor at higher concentrations of the ligand in the case of lithium. Thawing of the ether solution leads to a colour change from blue to green. A similar colour has been observed earlier for THF solutions of lanthanide complexes with the naphthalene dianion {575 nm for $[EuI(THF)_4]_2(\mu\text{-}C_{10}H_8)$ and 604 nm for $[LaI_2(THF)_3]_2(\mu\text{-}C_{10}H_8)$}.[6] One can suggest that in the diluted $Et_2O$ solution, at different temperatures, the mutual transition of two electronic isomers of the ligand takes place. In one of these forms the negative charge is, presumably, located mainly on the diimine function of the ligand (green) and in the second form on the naphthalene rings (deep blue). The latter form of the dpp-bian ligand may be considered as a dianion of the 1,8-disubstituted naphthalene. We suppose that transformation of the green dianion to the blue dianion is forced by the separation of the cation from the dianion by the solvent.

In order to find an experimental confirmation for this assumption we have tried to stabilise the dark blue form of $(dpp\text{-}bian)^{2-}$ using TMEDA as a solvent. Earlier, TMEDA was successfully used for the stabilisation of the lithium complex with the naphthalene dianion $[Li(TMEDA)]_2(\mu\text{-}C_{10}H_8)$.[7] The electronic absorption spectra of the reduction of dpp-bian with lithium in TMEDA are given in Figure 3. For the transition from $(dpp\text{-}bian)^{-}$ [432, 465 and 502 nm; Figure 3 (a), spectrum 2] to $(dpp\text{-}bian)^{2-}$ [Figure 3 (b), spectrum 3] the absorption that reflects the dianion formation, has a maximum at 612 nm and a shoulder at 645 nm. This spectrum corresponds to a dark blue colour of the solution. Further, this dark blue colour changes to a blue-green colour (spectrum 4). At that moment the absorption at 645 nm becomes most intense, and the maximum at 612 nm becomes a shoulder. We believe, that at the initial stages of the dianion formation, when its concentration is still very small, $Li^{+}_{2}(dpp\text{-}bian)^{2-}$ exists in solution as a solvent-separated ion pair. The negative charge of the dianion is located mostly on the naphthalene part of the molecule. Figure 3 (c) presents the transition from (dpp-

  

bian)$^{3-}$ to (dpp-bian)$^{4-}$. The absorption of the trianion (760 and 837 nm) gradually disappears in the sequence 5 → 6 → 7. We have not had an opportunity to record the spectrum of (dpp-bian)$^{4-}$ in the region of 1100−2000 nm, but we suggest that the absorption of (dpp-bian)$^{4-}$, which corresponds to the excitation of an electron from the HOMO of the tetraanion, shifts to the long-wavelength region (> 1100 nm).

### Molecular Structure of [Li$^+$(dpp-bian)$^-$(TMEDA)] (1)

Suitable crystals of **1** were obtained for X-ray structure determination by concentration of the TMEDA solution of **1**. The lithium atom in **1** has a distorted tetrahedral environment (Figure 4). The bite angles N(1)−Li(1)−N(2) and N(3)−Li(1)−N(4) are 87.03 and 83.90°, respectively. The lithium−dpp-bian bonds [Li(1)−N(1) 2.0365(18) and Li(1)−N(2) 2.0603(18) Å] are notably shorter than the lithium−TMEDA bonds [Li(1)−N(3) 2.1201(19) and Li(1)−N(4) 2.1701(19) Å]. The anionic character of the radical of the dpp-bian ligand in **1** is evident from the elongation of the C−N bond of the diimine moiety [C(1)−N(1) 1.3295(11) Å and C(11)−N(2) 1.3303(11) Å], compared with that of the neutral related ligand *p*-tol-bian [1.267(3) Å],[1b] the four-coordinate Pd$^{II}$ complex [(dpp-bian)PdCl(CH$_3$)][1b] (1.287 Å) and the five-coordinate Cu$^{II}$ complex [(dpp-bian)CuCl$_2$(AcOH)][8] (1.287 Å). On the other hand, the bonds C(1)−N(1) and C(11)−N(2) are very close to the respective bonds in [Na$^+$(dpp-bian)$^-$]$_2$ [1.3239(18) Å and 1.3326(19) Å][5] and substantially shorter than in the sodium complex with the dpp-bian dianion [Na$^+_2$(Et$_2$O)$_3$(dpp-bian)$^{2-}$] [1.387(4) and 1.386(4) Å].[5]

### ESR Spectroscopy of (dpp-bian)$^{n-}$[M$^+$]$_n$ (M = Li, Na; *n* = 1 or 3)

The mono- and trianions of dpp-bian consist of an unpaired electron making them detectable by ESR spectroscopy. Figures 5 and 6 represent the ESR spectra of (dpp-bian)$^-$ and (dpp-bian)$^{3-}$, respectively (upper spectra − observed; lower spectra − simulated). In a toluene solution [Na$^+$(dpp-bian)$^-$] reveals an ESR signal of six lines ($g$ = 2.0025) due to the coupling of the unpaired electron to two $^{14}$N nuclei ($I$ = 1, natural abundance 99.6%) and

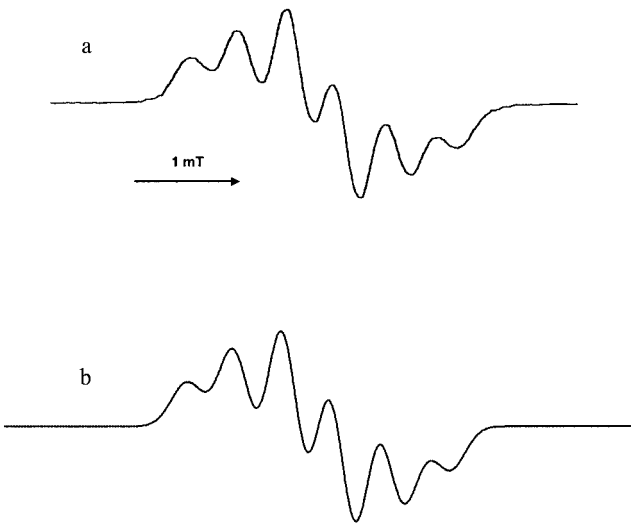


Figure 5. X-band ESR spectrum of [Na$^+$(dpp-bian)$^-$] in toluene at 285 K: (a) experimental; (b) simulated [$A_N$ = 0.46 (2 N), $A_{Na}$ = 017 (1 Na) mT, line width −0.31 mT)]

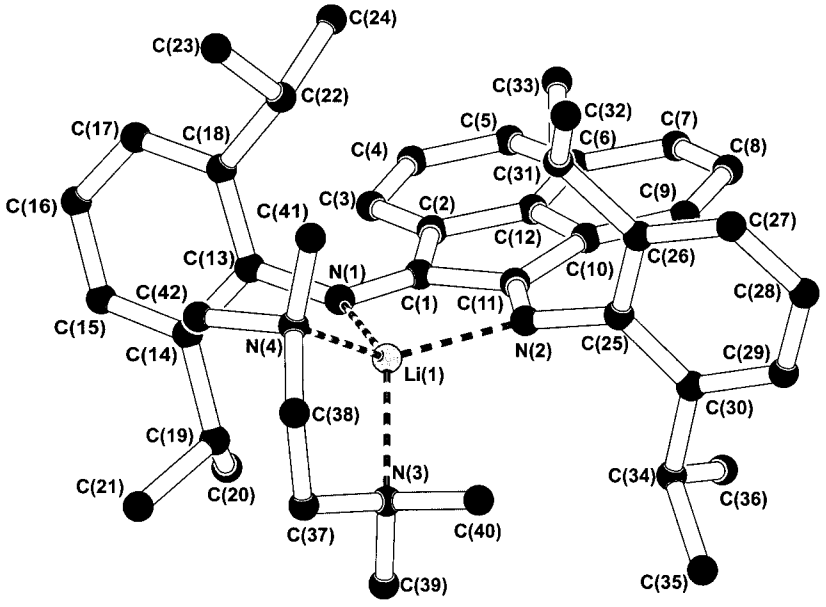


Figure 4. PLATON plot of the molecular structure of complex **1**; hydrogen atoms are omitted; selected bond lengths [Å] and angles [°]: Li(1)−N(1) 2.0365(18), Li(1)−N(2) 2.0603(18), Li(1)−N(3) 2.1201(19), Li(1)−N(4) 2.1701(19), N(1)−C(1) 1.3295(11), N(2)−C(11) 1.3303(11), N(1)−C(13) 1.4231(11), N(2)−C(25) 1.4206(11), C(1)−C(11) 1.4538(12), C(1)−C(2) 1.4768(12), C(2)−C(3) 1.3821(12), C(4)−C(5) 1.3766(15), C(2)−C(12) 1.4218(12), C(3)−C(4) 1.4216(13), C(5)−C(6) 1.4217(14), C(6)−C(7) 1.4263(14), C(6)−C(12) 1.3949(12), C(7)−C(8) 1.3747(15), C(8)−C(9) 1.4222(13), C(10)−C(12) 1.4219(12), C(9)−C(10) 1.3859(13), C(10)−C(11) 1.4793(12); N(1)−Li(1)−N(2) 87.03(7), N(3)−Li(1)−N(4) 83.90(7), N(2)−Li(1)−N(3) 110.21(9), N(1)−Li(1)−N(4) 113.44(9), N(2)−Li(1)−N(4) 135.97(9), N(1)−Li(1)−N(3) 133.90(9)

  

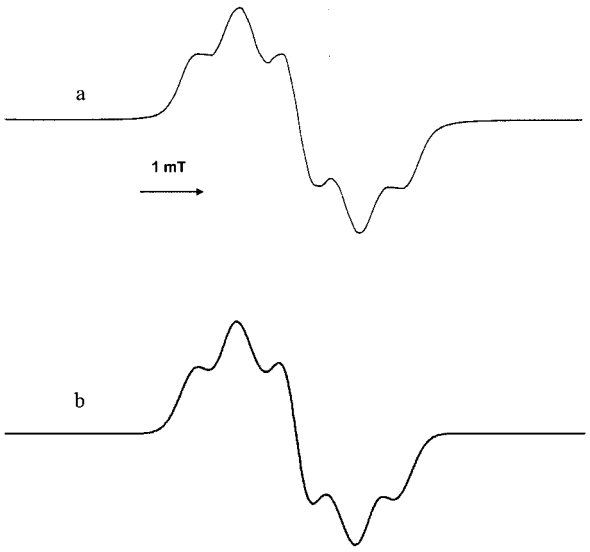


Figure 6. X-band ESR spectrum of $[Na^+{}_3(dpp\text{-}bian)^{3-}]$ in THF at 293 K: (a) experimental; (b) simulated [$A_H$ = 0.027 (2 H), 0.39 (2 H), 0.66 (2 H) mT, line width −0.42 mT)]

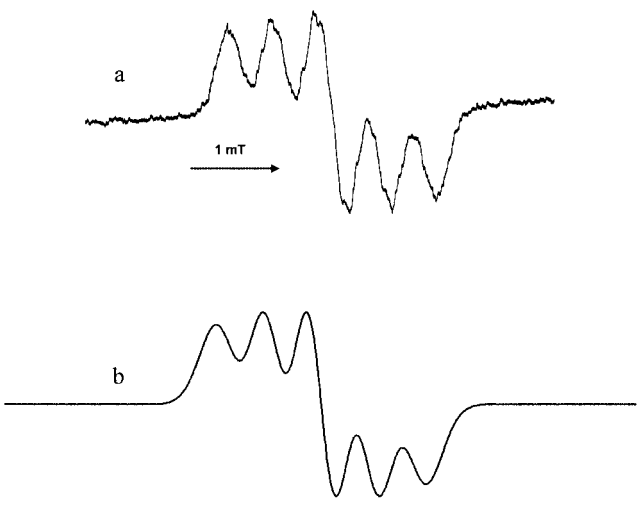


Figure 7. X-band ESR spectrum of $[Li^+(dpp\text{-}bian)^-]$ in TMEDA at 280 K: (a) experimental; (b) simulated [$A_N$ = 0.46 (2 N) mT, line width −0.42 mT)]

the $^{23}Na$ nucleus ($I$ = 3/2, natural abundance 100%). The hyperfine coupling constants [$A_N$ = 0.46 (2 N) and $A_{Na}$ = 0.17 (1 Na) mT)] of this signal indicate that: (i) the unpaired electron is mainly localized over the diimine part of the dpp-bian molecule and (ii) the complex exists in THF solution as a contact ion pair with the sodium atom being coordinated by two nitrogen atoms of the ligand. In contrast, the ESR signal of the trianion $[Na^+{}_3(dpp\text{-}bian)^{3-}]$ ($g$ = 2.0023) exhibits a hyperfine structure due to the coupling of the unpaired electron to three different pairs of $^1H$ nuclei [$A_H$ = 0.027 (2 H), $A_H$ = 0.39 (2 H) and $A_H$ = 0.66 (2 H) mT] (Figure 6). As there is no coupling to $^{14}N$ nuclei in the ESR signal of the trianion, we conclude that in $(dpp\text{-}bian)^{3-}$ the unpaired electron is delocalised over the naphthalene part of the dpp-bian ligand. These findings are in good agreement with the solid-state structures of $[Na^+(dpp\text{-}bian)^-]_2$ and $[Na^+{}_3(Et_2O)_2(dpp\text{-}bian)^{3-}]_2$.[5] In contrast to the sodium salt of the monoanion $(dpp\text{-}bian)^-$ the lithium derivative $[Li^+(dpp\text{-}bian)^-(TMEDA)]$ in TMEDA shows the ESR signal of five components (Figure 7). The hyperfine structure of this signal [$g$ = 2.0021, $A_N$ = 0.46 (2 N) mT] is caused by the coupling of the unpaired electron to only two $^{14}N$ nuclei, thus indicating that in TMEDA complex **1** exists as a solvent-separated ion pair. The ESR signal of $[Na^+(dpp\text{-}bian)^-]$ in THF is similar to that of complex **1** in TMEDA. However, in this spectrum there is a line of low intensity, which appears exactly in the middle of the quintuplet. The observed spectrum may be attributed to two overlapped signals of five and six lines. These signals correspond to the contact and solvent-separated ion pairs $[Na^+(dpp\text{-}bian)^-]$ (quintuplet) and $[Na(THF)_n]^+[dpp\text{-}bian]^-$ (sextuplet).

### $^1H$ NMR Spectroscopy of $(dpp\text{-}bian)^{n-}[M^+]_n$ (M = Na, $n$ = 2 or 4)

As anticipated, complexes $[Na^+{}_2(Et_2O)_3(dpp\text{-}bian)^{2-}]$ and $[Na^+{}_4(THF)_4(dpp\text{-}bian)^{4-}]_2$ are diamagnetic and therefore are detectable by NMR spectroscopy. The signals of the paramagnetic mono- and trianionic species, which appear in the solution due to disproportionation of $[Na^+{}_2(Et_2O)_3(dpp\text{-}bian)^{2-}]$, are not visible in the $^1H$ NMR spectrum because of their broadening. In the $^1H$ NMR solution spectrum in $C_6D_6$ the methyl groups of the isopropyl group appear as two doublets centred at δ = 1.41 ppm and for $[Na^+{}_2(Et_2O)_3(dpp\text{-}bian)^{2-}]$, due to hindered rotation about the aryl carbon−nitrogen bond, at δ = 1.33 ppm ($^3J$ = 8.0 Hz for both doublets). The signal for the four $H-C(CH_3)_2$ protons appears as a septuplet at δ = 3.85 ppm ($^3J$ = 8.0 Hz). The signals of the twelve aromatic protons are found in a relatively narrow region (δ = 7.32−6.51 ppm). Despite the extreme sensitivity of complex $[Na^+{}_4(THF)_4(dpp\text{-}bian)^{4-}]_2$ towards air and moisture, attempts to obtain its $^1H$ NMR spectrum were undertaken. The spectrum obtained in $[D_8]$THF revealed the presence of some impurities amounting to about 10%. These narrow signals are attributable to those observed for $[Na^+{}_2(Et_2O)_3(dpp\text{-}bian)^{2-}]$ in $C_6D_6$. The dominant signals in the spectrum are noticeably broadened, high-field shifted, and probably belong to the aromatic protons of the tetraanion (δ = 6.56, 6.45, 5.83, 4.64, 3.93, 2.83 ppm). The signal corresponding to the $H-C(CH_3)_2$ proton appears to be partly overlapping with the THF signal at δ = 3.60 ppm. The methyl protons of the isopropyl groups are observed as a broad single signal at δ = 0.91 ppm.

## Conclusion

Based on the UV/Vis spectroscopy data for $(dpp\text{-}bian)^{n-}[M^+]_n$ (M = Li, Na; $n$ = 1−4), we have established that in solution $(dpp\text{-}bian)^-$ and $(dpp\text{-}bian)^{2-}$ undergo disproportionation to species which can be oxidised and reduced by one electron. Nevertheless, as reported recently,[5] every reduced form of $(dpp\text{-}bian)^{n-}$ ($n$ = 1−4) may be isolated from solution in the individual state. The ESR spec-

  

troscopy data for lithium and sodium salts of the monoanion $(dpp\text{-}bian)^-$ show that these salts may exist in solution either as solvent-separated or contact ion pairs.

## Experimental Section

**General Remarks:** All manipulations were carried out under vacuum using Schlenk ampoules. Prior to use THF, toluene and diethyl ether were distilled from sodium/benzophenone. TMEDA was dried with lithium and condensed prior to use. 1,2-Bis[(2,6-diisopropylphenyl)imino]acenaphthene (dpp-bian) was prepared according to a published procedure.[8] The UV/Vis spectra were recorded with a Perkin−Elmer Lambda 25 spectrometer. Into the ampoule for UV/Vis spectroscopy, which contained sodium or lithium metal (10- to 20-fold excess calculated on the ligand), the solution of dpp-bian (20 mg, 0.04 mmol) in diethyl ether (40 mL) or in TMEDA (40 mL) was added. This ampoule was then sealed off under vacuum. The ESR spectra were recorded with a Bruker ER 200D-SRC spectrometer. The ESR signals were referenced to the signal of diphenylpicrylhydrazyl (DPPH, $g = 2.0037$).

**[Li(dpp-bian)(TMEDA)] (1):** A suspension of dpp-bian (0.5 g, 1.0 mmol) in TMEDA (30 mL) was added into a Schlenk ampoule, which contained lithium (1.0 g, 0.14 mmol). The mixture was stirred for 1 h. While stirring, the solution turned cherry-red. The solution was decanted from the lithium metal and then concentrated to 15 mL by evaporation of the solvent in vacuo on heating affording 0.34 g (55%) of **1** as dark red crystals. M.p. 199−201 °C. $C_{42}H_{56}LiN_4$ (623.85): calcd. C 80.72, H 9.11; found C 80.86, H 9.05.

**Single-Crystal X-ray Structure Determination of 1:** The data were collected with a SMART APEX diffractometer (graphite-monochromated, Mo-$K_\alpha$ radiation, ω- and ψ-scan technique, $\lambda = 0.71073$ Å). The structures were solved by direct methods using SHELXS-97[9] and were refined on $F^2$ using SHELXL-97[10]. All non-hydrogen atoms were refined anisotropically and the hydrogen atoms were placed in calculated positions and assigned to an isotropic displacement parameter of 0.08 Å$^2$. SADABS[11] was used to perform area-detector scaling and absorption corrections (max./min. transmission 0.9811/0.9688). The geometrical aspects of the structure were analysed using PLATON.[12] Data collection: crystal dimensions 0.50 × 0.40 × 0.30 mm, triclinic, $P\bar{1}$, $a = 10.5011(9)$ Å, $b = 13.2585(12)$ Å, $c = 14.0911(12)$ Å, $\alpha = 98.926(2)°$, $\beta = 104.293(2)°$, $\gamma = 91.076(2)°$, $V = 1874.8(3)$ Å$^3$, $Z = 2$, $\rho_{calcd.} = 1.105 \times 10^3$ kg m$^{-3}$, $\mu = 0.064$ mm$^{-1}$, $F(000) = 678$, $1.98° \le \theta \le 29.00°$, $-14 \le h \le 14$, $-18 \le k \le 17$, $-19 \le l \le 19$, 19549 data collected, 9690 unique data ($R_{int} = 0.0223$), 648 refined parameters, GOF($F^2$) = 1.030, final $R$ indices $\{R_1 = \Sigma F_o - F_c/\Sigma F_o$, $wR_2 = [\Sigma w(F_o^2 - F_c^2)^2/\Sigma w(F_o^2)^2]^{1/2}\}$ $R_1 = 0.0515$, $wR_2 = 0.1204$, max./min. residual electron density 0.422/−0.210 e·Å$^{-3}$. CCDC-210160 (**1**) contains the supplementary crystallographic data, which can be obtained free of charge at www.ccdc.cam.ac.uk/conts/retrieving.html or from the Cambridge Crystallographic Data Centre, 12 Union Road, Cambridge CB2 1EZ, UK; Fax: (internat.) + 44-1223/336-033; E-mail: deposit@ccdc.cam.ac.uk.

## Acknowledgments

This work was supported by the Russian Foundation for Basic Research (Grant RFBR No. 03-03-32246a). The spectroscopic studies were carried out in the Analytical Center of the IOMC RAS (Grant RFBR No. 00-03-40116).

[1] [1a] R. van Asselt, K. Vrieze, C. J. Elsevier, *J. Organomet. Chem.* **1994**, *480*, 27−40. [1b] R. van Asselt, C. J. Elsevier, W. J. J. Smeets, A. L. Spek, R. Benedix, *Recl. Trav. Chim. Pays-Bas* **1994**, *113*, 88−98. [1c] R. van Asselt, C. J. Elsevier, *Organometallics* **1994**, *13*, 1972−1980. [1d] R. van Asselt, C. J. Elsevier, W. J. J. Smeets, A. L Spek, *Inorg. Chem.* **1994**, *33*, 1521−1531. [1e] R. van Asselt, E. Rijnberg, C. J. Elsevier, *Organometallics* **1994**, *13*, 706−720. [1f] R. van Asselt, E. E. C. G. Gielens, R. E. Rulke, K. Vrieze, C. J. Elsevier, *J. Am. Chem. Soc.* **1994**, *116*, 977−985. [1g] R. van Asselt, E. E. C. G. Gielens, R. E. Rulke, C. J. Elsevier, *J. Chem. Soc., Chem. Commun.* **1993**, 1203−1204.

[2] [2a] M. W. van Laren, C. J. Elsevier, *Angew. Chem. Int. Ed.* **1999**, *38*, 3715−3717. [2b] R. van Belzen, H. Hoffmann, C. J. Elsevier, *Angew. Chem. Int. Ed. Engl.* **1997**, *36*, 1743−1745. [2c] E. Shirakawa, T. Hiyama, *J. Organomet. Chem.* **2002**, *653*, 114−121.

[3] [3a] D. Pappalardo, M. Mazzeo, S. Antinucci, C. Pellecchia, *Macromolecules* **2000**, *33*, 9483−9487. [3b] D. J. Tempel, L. K. Johnson, R. L. Huff, P. S. White, M. Brookhart, *J. Am. Chem. Soc.* **2000**, *122*, 6686−6700. [3c] D. P. Gates, S. A. Svejda, E. Onate, Ch. M. Killian, L. K. Johnson, P. S. White, M. Brookhart, *Macromolecules* **2000**, *33*, 2320−2334. [3d] S. A. Svejda, M. Brookhart, *Organometallics* **1999**, *18*, 65−74. [3e] M. Gasperini, F. Ragaini, S. Cenini, *Organometallics* **2002**, *21*, 2950−2957.

[4] I. L. Fedushkin, A. A. Skatova, V. A. Chudakova, G. K. Fukin, S. Dechert, H. Schumann, *Eur. J. Inorg. Chem.* **2003**, 3336−3346.

[5] I. L. Fedushkin, A. A. Skatova, V. A. Chudakova, G. K. Fukin, *Angew. Chem. Int. Ed.* **2003**, *42*, 3294−3298.

[6] I. L. Fedushkin, M. N. Bochkarev, H. Schumann, L. Esser, G. Kociok-Kohn, *J. Organomet. Chem.* **1995**, *489*, 145−151.

[7] J. J. Brooks, W. Rhine, G. D. Stucky, *J. Am. Chem. Soc.* **1972**, *94*, 7346−7351.

[8] A. A. Paulovicova, U. El-Ayaan, K. Shibayama, T. Morita, Y. Fukuda, *Eur. J. Inorg. Chem.* **2001**, 2641−2646.

[9] G. M. Sheldrick, *SHELXS-97, Program for the Solution of Crystal Structures*, Universität Göttingen, **1990**.

[10] G. M. Sheldrick, *SHELXL-97, Program for the Refinement of Crystal Structures*, Universität Göttingen, **1997**.

[11] G. M. Sheldrick, *SADABS, Program for Empirical Absorption Correction of Area Detector Data*, Universität Göttingen, **1996**.

[12] A. L. Spek, *PLATON, A Multipurpose Crystallographic Tool*, Utrecht University, **2000**.

Received June 7, 2003
Early View Article
Published Online November 6, 2003

  